

# Geometrical frustration, power law tunneling and non-local gauge fields from scattered light

Pavel P. Popov,<sup>1,\*</sup> Joana Fraxanet,<sup>1</sup> Luca Barbiero,<sup>2</sup> and Maciej Lewenstein<sup>1,3</sup>

<sup>1</sup>ICFO - Institut de Ciències Fotòniques, The Barcelona Institute of Science and Technology, 08860 Castelldefels (Barcelona), Spain

<sup>2</sup>Institute for Condensed Matter Physics and Complex Systems, DISAT, Politecnico di Torino, I-10129 Torino, Italy

<sup>3</sup>ICREA, Pg. Lluís Companys 23, ES-08010 Barcelona, Spain

(Dated: February 7, 2025)

Designing the amplitude and range of couplings in quantum systems is a fundamental tool for exploring a large variety of quantum mechanical effects. Here, we consider off-resonant photon scattering processes on a geometrically shaped molecular cloud. Our analysis shows that such a setup is properly modeled by a Bose-Hubbard Hamiltonian where the range, amplitude and sign of the tunneling processes of the scattered photonic modes can be accurately tuned. Specifically, by varying the molecular distribution, we demonstrate that different configurations characterized by geometrical frustration, long-range power law hopping processes, and non-local gauge fields can be achieved. Our results thus represent a powerful and alternative approach to perform an accurate Hamiltonian engineering of quantum systems with non trivial coupling structures.

*Introduction.*— Non-local couplings [1] are key ingredients to explore quantum mechanical effects which can deeply influence the entanglement [2, 3], symmetry [4, 5], and out-of-equilibrium [6, 7] properties of complex quantum systems. In addition, when specifically shaped non-local couplings can generate the celebrated phenomenon of geometrical frustration [8]. As known, the latter can have the fundamental role of allowing for the appearance of interesting states of matter characterized by various kind of spontaneously symmetry breakings [9, 10] or topological order [11]. Interestingly, alternative and fundamental resources to achieve frustration or, generally, quantum phases with broken symmetries or topological order are classical gauge fields. These latter, in addition to representing one of the most fundamental concepts in quantum mechanics [12, 13], are a timely research subject [14] for different communities ranging from ultracold atomic systems [15–21] and solid state [22] to photonic [23–26] and mechanical systems [27–29].

In this paper, we demonstrate that the three fundamental aspects — long-range couplings, geometrical frustration, and classical gauge fields — can be engineered through the controlled scattering of photons within a carefully designed molecular geometry. Specifically, we first design a setup where light in form of a Gaussian beam is scattered off-resonantly from a molecular cloud. This scheme allows deriving an effective Bose-Hubbard Hamiltonian [30, 31] where the scattered modes represent the elementary constituents of the considered physical systems. Notably, in such setup the sign, amplitude and range of the interparticle couplings can be accurately tuned by shaping the geometry of the molecular cloud. Contrary to Ref. [32] where the control parameter is the size of the molecular cloud, we utilize different distribution profiles and find that homogeneous lattice geometries can be efficiently realized. Within this approach, we first prove that the scattered modes can be confined to an effective triangular ladder geometry characterized by geometrical frustration. We then show that a similar manipulation of the molecular distribution generates highly non-local terms in the form of long-range hopping processes of the scattered modes. Here, we can indeed achieve

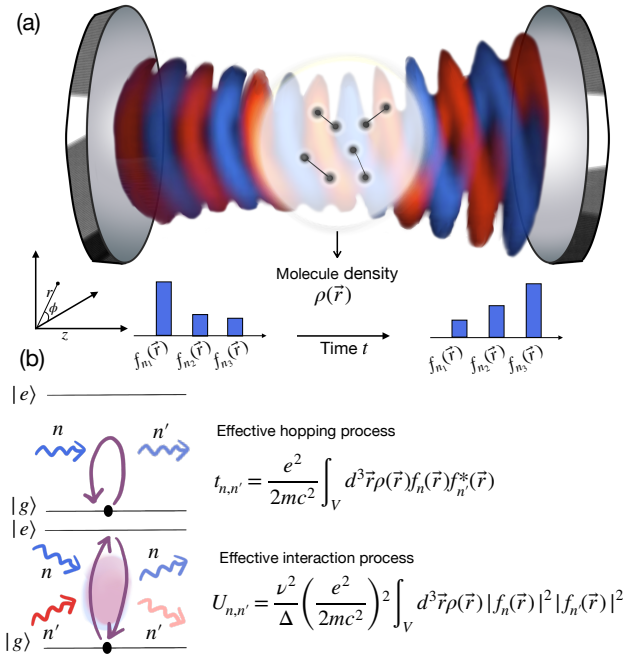


Figure 1. **Physical Setup.** (a) A Gaussian beam represented by blue and red patterns illuminates a geometrically shaped molecular cloud in a cavity with molecule density  $\rho(\vec{r})$ . The beam frequency is tuned so that off-resonant scattering is the dominant light-matter interaction. Scattering dynamically alters the beam's mode decomposition in a suitably chosen basis with decomposition coefficients  $f_n(\vec{r})$ , e.g., the Laguerre-Gaussian basis. (b) To second-order perturbation theory, the effective bosonic Hamiltonian features tunable long-range hoppings  $t_{n,n'}$  and density-density interactions  $U_{n,n'}$ . The geometry of the molecular cloud controls the sign and phase of the hopping and interaction amplitudes.

regimes where the tunneling amplitude of scattered modes follow a power law decay whose decay exponent can be tuned to basically any value. Notably, this feature represents a key aspect for quantum information purposes [33, 34]. Finally, we show that when the profile of the molecular cloud is rotated with respect to the profile of the incident beam, gauge fields affecting the dynamic of the scattered modes

can be generated. Notably, we demonstrate that our scheme not only makes it possible for an accurate tuning of the fields value but, thanks to higher non-homogeneity of the molecular cloud, the gauge fields can also become highly non-local, i.e. they can extend over different effective triangular plaquettes thus proving, even more, the relevance of our results.

*Physical setup and Hamiltonian engineering.*— The setup, as depicted in Fig. 1 (a), consists of a cavity where the molecules are confined in a cylindrical geometry, with a density distribution  $\rho(\vec{r})$ . A single frequency Gaussian beam  $\omega_0$  is focused on the molecular cloud, so that off-resonant scattering of the photons on the molecules takes place. The frequency of the photons  $\omega_0$  can be tuned far away from typical electronic transitions, so that only off-resonant processes are relevant. We further assume that the light interacts with the valence electron in each molecule. The minimal Hamiltonian that captures all these processes reads [35]

$$\mathcal{H} = \sum_{\alpha} \frac{1}{2m} \left( \vec{p}_{\alpha} - \frac{e}{c} \vec{A}(\vec{r}_{\alpha}) \right)^2 + V(\vec{r}_{\alpha}, \vec{R}_{\alpha}) + \sum_n \omega_n b_n^{\dagger} b_n, \quad (1)$$

where  $m, e$  are the electron mass and charge and  $c$  is the velocity of light. In Eq. (1),  $V(\vec{r}_{\alpha}, \vec{R}_{\alpha})$  is the potential each electron feels in the molecule,  $\vec{r}_{\alpha}$  is the position operator of the electron,  $\vec{p}_{\alpha}$  is the corresponding canonical momentum, and  $\vec{R}_{\alpha}$  is the position of the molecule. In this expression, the index  $\alpha$  is enumerating the different molecules, and the index  $n$  accounts for the different photon modes in the expansion of the electromagnetic (EM) part of the Hamiltonian. Since we consider a Gaussian beam, the expansion has to be performed in a set of eigenmodes of the paraxial Helmholtz equation, for more details, see Supplemental Material (SM) [36]. Furthermore, in Eq. (1)  $\vec{A}(\vec{r}_{\alpha})$  denotes the vector potential of the EM field and  $b_n$  is the annihilation operator of the mode with index  $n$ . Importantly, here the energy of each mode is given by  $\omega_n = \omega_0 + \delta_n$ , where  $\delta_n$  are small corrections to the frequency of the Gaussian beam. Neglecting the term  $\vec{p}_{\alpha} \cdot \vec{A}(\vec{r}_{\alpha}) + \vec{A}(\vec{r}_{\alpha}) \cdot \vec{p}_{\alpha}$  in Eq. (1), as the frequency of the incoming beam is chosen to be off-resonant with the electronic transitions in the molecule, we rewrite the Hamiltonian as follows:

$$\mathcal{H} = \underbrace{\sum_{\alpha} \frac{1}{2m} \vec{p}_{\alpha}^2 + V(\vec{r}_{\alpha}, \vec{R}_{\alpha})}_{H_0} + \underbrace{\sum_{\alpha} \frac{e^2}{2mc^2} \vec{A}(\vec{r}_{\alpha})^2 + \sum_n \delta_n b_n^{\dagger} b_n}_{H_1}, \quad (2)$$

where we have dropped constant terms. The wave function of the electronic structure in each molecule can be obtained

from the first part of the Hamiltonian -  $H_0$ . We approximate this structure by a two-level system whose ground state  $|g_{\alpha}\rangle$  and excited state  $|e_{\alpha}\rangle$  are separated by an energy gap  $E = \Delta$  and we assume that all molecules are prepared in their ground state. The second part of the Hamiltonian,  $H_1$ , describes the evolution of the mode decomposition of the Gaussian beam, when interacting with the scatterers, and can be treated as a perturbation of  $H_0$ .

The first-order correction to the unperturbed part  $H_0$  comes from the projection of  $H_1$  onto the ground state of  $H_0$ , which is given by the product:

$$|G\rangle = \prod_{\alpha} |g_{\alpha}\rangle \otimes |N\text{photons}\rangle, \quad (3)$$

where we assumed that the total number of photons  $N$  does not change (no photon losses) [37]. Therefore, the first order correction is

$$\langle G | H_1 | G \rangle = \frac{e^2}{2mc^2} \sum_{\alpha} \langle g_{\alpha} | \vec{A}(\vec{r}_{\alpha})^2 | g_{\alpha} \rangle. \quad (4)$$

The second-order perturbation term is a contribution from a virtual transition to the excited state of the electron in each molecule, which reads

$$-\frac{1}{\Delta} \sum_{\alpha} |\langle G | H_1 | E_{\alpha} \rangle|^2 = -\frac{1}{\Delta} \left( \frac{e^2}{2mc^2} \right)^2 \sum_{\alpha} |\langle g_{\alpha} | \vec{A}(\vec{r}_{\alpha})^2 | e_{\alpha} \rangle|^2, \quad (5)$$

where we denoted as  $|E_{\alpha}\rangle$  the state in which the  $\alpha$ -th molecule is excited and all the other molecules not. In order to simplify the calculations, we rewrite the off-diagonal element as proportional to the diagonal one

$$|\langle g_{\alpha} | \vec{A}(\vec{r}_{\alpha})^2 | e_{\alpha} \rangle|^2 = \nu^2 \langle g_{\alpha} | \vec{A}(\vec{r}_{\alpha})^2 | g_{\alpha} \rangle^2 \quad (6)$$

with proportionality factor  $\nu$  dependent on the molecular structure. The factor  $\nu$  can be calculated for specific molecules, knowing the ground and the excited state wave functions.

We proceed by expanding the vector potential in the creation and annihilation operators of suitably chosen photon modes. In case of a cylindrical symmetry, suitable choice of a basis for the photon modes are the Laguerre-Gauss (LG) polynomials [38]. The corresponding photon modes have two quantum numbers, the azimuthal index  $l$  and the radial index  $p$ , thus  $n$  becomes a multi-index:  $n \sim (l, p)$ . The vector potential expressed in this basis is

$$\vec{A}(\vec{r}, t) = \sum_{l,p} \vec{\epsilon} f_{l,p}(\vec{r}, t) e^{i\omega_0(z/c-t)} b_{l,p}^{\dagger} + \text{h.c.}, \quad (7)$$

where  $\vec{e}$  is the polarization vector (e.g. for circular polarization,  $\vec{e} = (\vec{x} - i\vec{y})/\sqrt{2}$ ),  $b_{l,p}$  is the annihilation operator and  $f_{l,p}(\vec{r}, t) \approx f_{l,p}(\vec{r})$  ( $\delta_n$  are small) is the spatial dependence of the  $(l, p)$ -th LG mode (see SM for details). Substituting Eq. (7) in Eq. (4) and in Eq. (5) yields the effective time-independent Bose-Hubbard Hamiltonian [30, 31] for the transverse LG modes:

$$\begin{aligned} \mathcal{H}_{\text{eff}} = & \sum_n \mu_n b_n^\dagger b_n + \sum_{n,n'} [|t_{n,n'}| e^{i\theta_{n,n'}} b_n b_{n'}^\dagger + \text{h.c.}] \\ & - \sum_{n,n'} U_{n,n'} [3b_n^\dagger b_n + 4b_n^\dagger b_n b_{n'}^\dagger b_{n'}], \end{aligned} \quad (8)$$

where the coefficients  $\mu$ ,  $t$  and  $U$  correspond to on-site chemical potential, hopping amplitudes and the strength of density-density interactions, respectively. Crucially, all these terms depend on the geometry of the molecular cloud as follows

$$\mu_n = \frac{e^2}{2mc^2} \int_V d^3\vec{r} \rho(\vec{r}) |f_n(\vec{r})|^2 + \delta_n, \quad (9)$$

$$t_{n,n'} = \frac{e^2}{2mc^2} \int_V d^3\vec{r} \rho(\vec{r}) f_n(\vec{r}) f_{n'}^*(\vec{r}), \quad (10)$$

$$U_{n,n'} = \frac{\nu^2}{\Delta} \left( \frac{e^2}{2mc^2} \right)^2 \int_V d^3\vec{r} \rho(\vec{r}) |f_n(\vec{r})|^2 |f_{n'}(\vec{r})|^2. \quad (11)$$

It is now important to remark the key aspects characterizing Eq. (8). First, the hopping coefficients  $t_{n,n'} = |t_{n,n'}| e^{i\theta_{n,n'}}$  are in general complex numbers. This is, as we elaborate in the remainder of this Letter, crucial for engineering frustration and effective classical gauge fields. Second, the interaction processes induced by the second order expansion can result either attractive when perturbation theory is performed around the molecular ground state, as in Eq. (8), or repulsive by considering perturbation theory around the molecular excited state  $\prod_\alpha |e_\alpha\rangle$ . Third, the prefactor  $\nu^2/\Delta$  of the interacting terms involves characteristics that depend on the type of molecules used as scatterers. Therefore, potentially different interaction ranges can be explored by considering suitable molecules.

*Manipulation of couplings by geometrical shaping:*— In this section, we demonstrate the high level of versatility encoded in the effective Bose-Hubbard Hamiltonian in Eq. (8). Our particular choice for the density of the molecular cloud as a function of the position in cylinder coordinates  $\vec{r} = (r, \phi, z)$  reads

$$\begin{aligned} \rho(r, \phi, z) = & \theta(r)\theta(R-r) \sum_{k=0}^{N_c} c_k \cos(k\phi + \varphi_k) \\ & \times \theta(z - z_1)\theta(z_2 - z). \end{aligned} \quad (12)$$

Here, the amplitudes  $c_k$ , the phases  $\varphi_k$  and the number of cosine-terms  $N_c$  are free parameters while the spatial extent along the  $z$ -direction  $z_1 - z_2$  and the radial extent  $R$  are set by the size of the cavity, in which the molecules are confined.

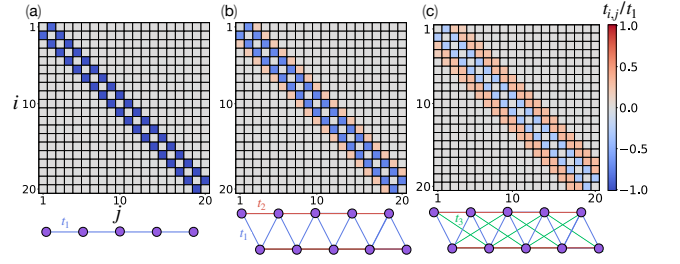


Figure 2. **Effective geometries.** (a) Purely 1D geometry induced by fixing  $c_1 = 1$ ,  $\varphi_1 = 0.9\pi$  and  $c_i = 0$  for  $\forall i > 1$ . (b) Effective frustrated triangular geometry obtained by fixing  $c_1 = 3/4$ ,  $c_2 = 1/4$ ,  $\varphi_1 = 0.9\pi$ ,  $\varphi_2 = 1.1\pi$  and  $c_i = 0$  for  $\forall i > 2$ . (c) Effective frustrated triangular geometry with hopping amplitudes connecting up to three sites obtained by fixing  $c_1 = 1/3$ ,  $c_2 = 1/3$ ,  $c_3 = 1/3$ ,  $\varphi_1 = 0.9\pi$ ,  $\varphi_2 = 1.1\pi$ ,  $\varphi_3 = 1.02\pi$  and  $c_i = 0$  for  $\forall i > 3$ .

The simple  $\phi$ -dependence of the LG modes,  $f_{l,p}(\phi) \sim \exp(-il\phi)$ , allows us to choose a molecular density as in Eq. (12) that decouples LG modes with different  $p$ -number. Therefore, if the Gaussian beam is initialized in the  $p = 0$  sector, it remains confined in this sector during time evolution. In what follows, we enumerate the modes through their azimuthal index,  $n \equiv (l, 0)$ .

Importantly, the coefficients  $c_k$  and  $\varphi_k$  in the  $\phi$ -dependence of  $\rho(\vec{r})$  serve as control parameters for the hopping amplitudes  $t$  and the interaction strengths  $U$ . In this regard, there are few key observations that need to be made. First, each  $c_k$  controls the hopping amplitude between  $n$ -th and  $(n+k)$ -th mode for all  $n$  under consideration, thus assuring translational invariance of the effective Hamiltonian. This feature is in crucial difference to previous proposals, where translational invariance is much harder to control [32, 39]. Second, the number  $N_c$  of non-zero coefficients  $c_k$  sets the range of the hoppings, allowing also for up to  $N_c$ -th nearest neighbor, i.e. all to all, hoppings. Third, the complex phase of each hopping amplitude  $\theta_{n,n+k}$  is fully controlled by the phase  $\varphi_k$ . Fourth, the interaction strengths  $U$  are controlled also by  $c_k$ , but are independent of  $\varphi_k$ .

To this end, we note that the non-negativity of the density of molecules  $\rho(r, \phi, z) \geq 0$  in any point of space imposes constraints on the sum of coefficients  $\sum_k c_k$ . In the case  $\alpha_k = 0 \forall k$ , the constraint is simply  $\sum_{k \geq 1} c_k \leq 1$ . The rest of this Letter is dedicated to exploring configurations with specifically shaped non-trivial interparticle couplings. In particular, we show that a Bose-Hubbard Hamiltonians with extended tunneling range can be engineered by controlling the coefficients  $c_k$ , for  $k \in \{0, \dots, N_c\}$  in Eq. (12).

*Effective geometrical frustration:*— Within the described approach, a Bose-Hubbard model featuring nearest neighbor hopping only, see Fig 2(a), arises by choosing the coefficients in Eq. (12) to be  $c_0 = c_1 = 1$  and  $c_k = 0 \forall k \geq 2$ . By switching on the second coefficient  $c_2$ , we turn on the next-nearest neighbor hopping term in the Hamiltonian (8). This corresponds to an effective triangular ladder geometry, see Fig. 2(b), thus showing that our implementation allows for

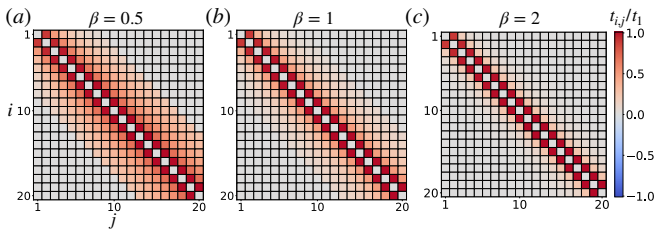


**Figure 3. Power-law decay of the hopping amplitudes** The matrix  $t_{i,j}$  representing the hopping amplitudes in the kinetic Hamiltonian as in Eq. (13) for three different values of the exponent: (a)  $\beta = 0.5$ , (b)  $\beta = 1$  and (c)  $\beta = 2$ . The first seven hopping amplitudes ( $i - 7 \leq j \leq i + 7$ ) are tuned to be non-zero by switching on the corresponding  $c$ -coefficients in the density of the scatterers.

realizations beyond purely 1D systems. As mentioned in the previous section, the relative strength and sign of the nearest to next-nearest neighbor hopping is fully tunable by the ratio  $c_2/c_1$  and  $\varphi_{1,2}$  respectively. In such a simple way, we can then achieve regimes where geometrical frustration occurs by fixing  $t_1, t_2 > 0$  or, as reported in Fig. 2(b),  $t_1 < 0, t_2 > 0$ , see [40] for an analogy with spin chains. It is important to remark that contrary to ultracold atomic systems where engineering frustration [17, 41] requires potentially detrimental fast periodic drivings, here frustration is created just through geometry manipulations. Moreover, frustration in addition to the present weak interactions  $U_{n,n'}$  can give rise to chiral superfluidity which represents an interesting and exotic state of matter predicted to appear both in high energy [42] and condensed matter [43–50] systems. Interestingly, the range of hopping can be further extended by turning on  $c_3$ . In such a way, see Fig. 2(c), we get an effective triangular frustrated system where up to tree effective lattice sites are connected. Crucially, this latter example represents the building block of purely two dimensional geometries displaying spin liquid phases [51, 52].

*Power law tunneling processes:*— By switching on further coefficients  $c_i$  and adjusting their value, one can engineer effective power-law decaying hopping terms

$$t_{n,m} \propto \frac{1}{|n-m|^\beta} \quad (13)$$

with a power  $\beta$  that can be freely tuned. In order to achieve that, one needs to tune the relative strength of the coefficients  $c_i$  accordingly:  $c_i \sim i^{-\beta}$ . Fig. 3 clearly shows that  $\beta$  can acquire different values in a very controlled way so to reproduce both almost local, i.e  $\beta \geq 1$ , and highly non-local, i.e  $\beta \leq 1$ , regimes. In this regard, it is important to underline that while similar features have been achieved in trapped-ion quantum simulators mimicking spin-1/2 models [53–57], in our case the tunability of  $\beta$  applies to systems with an extended local Hilbert space.

*Classical gauge fields:*— The versatility characteristic of our approach becomes even more spectacular when considering rotations of the hoppings in the complex plane. Here, as shown in Fig. 4 artificial gauge fields take place. Contrary to

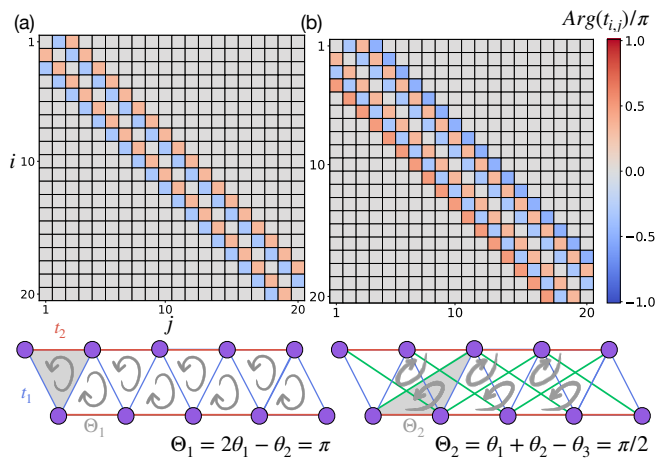


**Figure 4. Classical gauge fields.** (a) The complex phase of the nearest ( $t_1$ ) and next-nearest ( $t_2$ ) neighbor hopping can be tuned so that going around a plaquette on the triangular ladder, the bosonic particle acquires a phase of  $\Theta_1 = \pi$ . (b) By switching on the next-to-next nearest neighbor hopping ( $t_3$ ), another plaquette, defined by  $t_1, t_2$  and  $t_3$  can be identified. Choosing the complex phase of  $t_3$  accordingly, a phase shift of  $\Theta_2 = \pi/2$  by going around this second plaquette can be induced.

other setups like cold atomic [14, 16], solid state [22], photonic [25] and optomechanical [29] settings, our setup allows for arbitrary adjusting of the Peierls phase by one control parameter – the relative orientation between the molecular cloud and the LG modes. More specifically, the Peierls phase acquired by the photon hopping from the  $n$ -th LG mode to the  $(n+k)$ -th LG mode is given by the sum of the azimuthal phase difference between the two modes and the phase  $\varphi_k$ . The ability to tune  $\varphi_k$  arbitrarily by simply rotating the corresponding cos-component in the density of the molecular cloud (see Eq. (12)) around the  $z$ -axis, allows us to engineer arbitrary Peierls phases for each hopping independently. In particular, the engineered Peierls phases are strictly translationally invariant, as they only depend on  $k$  and not on  $n$ .

In Fig. 4 (a) we show the complex phase of the kinetic part of the effective Hamiltonian, chosen so that in the triangular ladder geometry, a phase of  $\Theta_1 = \pi$  is acquired by going around a plaquette. In Fig. 4 (b) we add one layer of complexity by introducing a next-to-next nearest neighbor hopping with a complex amplitude, so that two different phases –  $\Theta_1 = \pi$  and  $\Theta_2 = \pi/2$  are acquired, dependent on the triangle. Specifically here the generated gauge fields can become effectively long-range as they can extended over different triangular plaquettes. As we underline, this unique feature can be made by controlling the density profile of the molecular cloud thus further proving the conceptual simplicity of our designed setup.

*Conclusions and outlook.*— We studied the behavior of photons scattering off-resonantly from a molecular cloud. In such a context, we derived a highly versatile Bose-Hubbard model where the elementary constituents are represented by the scattered photonic modes. Crucially, we demonstrated

that the molecular distribution represents a fundamental control parameter in order to achieve interesting configurations. Specifically, we first proved that by properly shaping the molecular geometry the range of the tunneling amplitude can extend beyond nearest-neighbor sites. In addition, we showed that the sign of the hopping processes can be adjusted so that effective geometrical frustration naturally emerges. In this regard, we remark that configurations where geometrical frustration coexists with local and non-local interactions, as in our model, have been recently proposed as the ideal playground to explore states of matter characterized by chiral order [50] and exotic phase transitions [49]. In addition to these important aspects, we also proved that the shape of the tunneling processes can be modeled at will. As an important example, we designed long-range tunneling processes that decay following a power-law scaling. Importantly, we further demonstrated that by altering the azimuthal angle dependence of the molecular density, the exponent governing the power law decay can take basically any value. As very recently proved [33, 34], this point represents a fundamental tool required to achieve the so called Grover’s optimum [58, 59] and, generally, an efficient quantum random walk. Finally, we further showed that by rotating the molecular cloud with respect to the incident laser beams, the scattered modes can acquire a complex phase, i.e. a classical gauge field, at each tunneling event. Importantly, our approach allows for configurations in which the gauge fields can also extend beyond the nearest-neighbor approximation. Crucially, this latter represents a fundamental resource needed to create paradigmatic topological phases [60]. Finally, we stress that our work naturally motivates very promising and fundamental research directions. In particular, the search for specific molecules with a small gap and well-separated ground and first excited vibrational state from the rest of the spectrum can in principle open the path towards the exploration of strongly interacting photonic regimes [61, 62]. In conclusion, our results represent an alternative and powerful approach to investigate novel quantum mechanical effects emerging in presence of geometrical frustration, power law couplings and gauge fields.

*Acknowledgments.*— We warmly thank S. Asban for his contribution in the initial phase of this project. We also thank I. Carusotto and O. Firstenberg for discussions. ICFO-QOT group acknowledges support from: European Research Council AdG NOQIA; MCIN/AEI (PGC2018-0910.13039/501100011033, CEX2019-000910-S/10.13039/501100011033, Plan National FIDEUA PID2019-106901GB-I00, Plan National STAMEENA PID2022-139099NB, I00, project funded by MCIN/AEI/10.13039/501100011033 and by the “European Union NextGenerationEU/PRTR” (PRTR-C17.I1), FPI); QUANTERA MAQS PCI2019-111828-2; QUANTERA DYNAMITE PCI2022-132919, QuantERA II Programme co-funded by European Union’s Horizon 2020 program under Grant Agreement No 101017733; Ministry for Digital Transformation and of Civil Service of the Spanish Government through the QUANTUM ENIA project call -

Quantum Spain project, and by the European Union through the Recovery, Transformation and Resilience Plan - NextGenerationEU within the framework of the Digital Spain 2026 Agenda; Fundació Cellex; Fundació Mir-Puig; Generalitat de Catalunya (European Social Fund FEDER and CERCA program, AGAUR Grant No. 2021 SGR 01452, Quantum-CAT U16-011424, co-funded by ERDF Operational Program of Catalonia 2014-2020); Barcelona Supercomputing Center MareNostrum (FI-2023-3-0024); Funded by the European Union. Views and opinions expressed are however those of the author(s) only and do not necessarily reflect those of the European Union, European Commission, European Climate, Infrastructure and Environment Executive Agency (CINEA), or any other granting authority. Neither the European Union nor any granting authority can be held responsible for them (HORIZON-CL4-2022-QUANTUM-02-SGA PASQuanS2.1, 101113690, EU Horizon 2020 FET-OPEN OPTologic, Grant No 899794, QU-ATTO, 101168628), EU Horizon Europe Program (This project has received funding from the European Union’s Horizon Europe research and innovation program under grant agreement No 101080086 NeQST-Grant Agreement 101080086 — NeQST); ICFO Internal “QuantumGaudi” project; European Union’s Horizon 2020 program under the Marie Skłodowska-Curie grant agreement No 847648; P.P.P. acknowledges also support from the “Secretaria d’Universitats i Recerca del Departament de Recerca i Universitats de la Generalitat de Catalunya” under grant 2024 FI-3 00390, as well as the European Social Fund Plus. L. B. acknowledges financial support within the DiQut Grant No. 2022523NA7 funded by European Union– Next Generation EU, PRIN 2022 program (D.D. 104- 02/02/2022 Ministero dell’Universit’a e della Ricerca).

---

\* [pavel.popov@icfo.eu](mailto:pavel.popov@icfo.eu)

- [1] N. Defenu, T. Donner, T. Macrì, G. Pagano, S. Ruffo, and A. Trombettoni, Long-range interacting quantum systems, *Rev. Mod. Phys.* **95**, 035002 (2023).
- [2] J. Eisert, M. van den Worm, S. R. Manmana, and M. Kastner, Breakdown of quasilocality in long-range quantum lattice models, *Phys. Rev. Lett.* **111**, 260401 (2013).
- [3] Z.-X. Gong, M. Foss-Feig, F. G. S. L. Brandão, and A. V. Gorshkov, Entanglement area laws for long-range interacting systems, *Phys. Rev. Lett.* **119**, 050501 (2017).
- [4] P. Bruno, Absence of spontaneous magnetic order at nonzero temperature in one- and two-dimensional heisenberg and  $XY$  systems with long-range interactions, *Phys. Rev. Lett.* **87**, 137203 (2001).
- [5] M. F. Maghrebi, Z.-X. Gong, and A. V. Gorshkov, Continuous symmetry breaking in 1d long-range interacting quantum systems, *Phys. Rev. Lett.* **119**, 023001 (2017).
- [6] P. Hauke and L. Tagliacozzo, Spread of correlations in long-range interacting quantum systems, *Phys. Rev. Lett.* **111**, 207202 (2013).
- [7] P. Richerme, Z.-X. Gong, A. Lee, C. Senko, J. Smith, M. Foss-Feig, S. Michalakis, A. V. Gorshkov, and C. Monroe, Non-local propagation of correlations in quantum systems with long-range

- interactions, *Nature* **511**, 198 (2014).
- [8] C. Lhuillier and G. Misguich, Frustrated quantum magnets, in *High Magnetic Fields: Applications in Condensed Matter Physics and Spectroscopy*, edited by C. Berthier, L. P. Lévy, and G. Martinez (Springer Berlin Heidelberg, Berlin, Heidelberg, 2001) pp. 161–190.
- [9] A. A. Nersisyan, A. O. Gogolin, and F. H. L. Eßler, Incommensurate spin correlations in spin-1/2 frustrated two-leg heisenberg ladders, *Phys. Rev. Lett.* **81**, 910 (1998).
- [10] C. Lacroix, P. Mendels, and F. Mila, *Introduction to frustrated magnetism* (Springer Ser. Solid-State Sci, 2011).
- [11] S. Fujimoto, Hall effect of spin waves in frustrated magnets, *Phys. Rev. Lett.* **103**, 047203 (2009).
- [12] Y. Aharonov and D. Bohm, Significance of electromagnetic potentials in the quantum theory, *Phys. Rev.* **115**, 485 (1959).
- [13] M. V. Berry, Quantal phase factors accompanying adiabatic changes, *Proceedings of the Royal Society of London. A. Mathematical and Physical Sciences* **392**, 45 (1984), <https://royalsocietypublishing.org/doi/pdf/10.1098/rspa.1984.0023>.
- [14] M. Aidelsburger, S. Nascimbene, and N. Goldman, Artificial gauge fields in materials and engineered systems, *Comptes Rendus. Physique* **19**, 394 (2018).
- [15] M. Aidelsburger, M. Atala, S. Nascimbène, S. Trotzky, Y.-A. Chen, and I. Bloch, Experimental realization of strong effective magnetic fields in an optical lattice, *Phys. Rev. Lett.* **107**, 255301 (2011).
- [16] J. Dalibard, F. Gerbier, G. Juzeliūnas, and P. Öhberg, Colloquium: Artificial gauge potentials for neutral atoms, *Rev. Mod. Phys.* **83**, 1523 (2011).
- [17] J. Struck, C. Ölschläger, M. Weinberg, P. Hauke, J. Simonet, A. Eckardt, M. Lewenstein, K. Sengstock, and P. Windpassinger, Tunable gauge potential for neutral and spinless particles in driven optical lattices, *Phys. Rev. Lett.* **108**, 225304 (2012).
- [18] M. Aidelsburger, M. Atala, M. Lohse, J. T. Barreiro, B. Paredes, and I. Bloch, Realization of the Hofstadter Hamiltonian with ultracold atoms in optical lattices, *Phys. Rev. Lett.* **111**, 185301 (2013).
- [19] N. Goldman and J. Dalibard, Periodically driven quantum systems: Effective Hamiltonians and engineered gauge fields, *Phys. Rev. X* **4**, 031027 (2014).
- [20] N. Goldman, J. C. Budich, and P. Zoller, Topological quantum matter with ultracold gases in optical lattices, *Nature Physics* **12**, 639–645 (2016).
- [21] D.-W. Zhang, Y.-Q. Zhu, Y. X. Zhao, H. Yan, and S.-L. Zhu, Topological quantum matter with cold atoms, *Advances in Physics* **67**, 253–402 (2018).
- [22] M. Vozmediano, M. Katsnelson, and F. Guinea, Gauge fields in graphene, *Physics Reports* **496**, 109 (2010).
- [23] J. Joannopoulos, S. Johnson, J. Winn, and R. Meade, *Photonic crystals: Molding the flow of light*, in *Photonic Crystals* (Princeton University Press, United States, 2011).
- [24] R. O. Umucalılar and I. Carusotto, Artificial gauge field for photons in coupled cavity arrays, *Phys. Rev. A* **84**, 043804 (2011).
- [25] M. HAFEZI, Synthetic gauge fields with photons, *International Journal of Modern Physics B* **28**, 1441002 (2014), <https://doi.org/10.1142/S0217979214410021>.
- [26] T. Ozawa, H. M. Price, A. Amo, N. Goldman, M. Hafezi, L. Lu, M. C. Rechtsman, D. Schuster, J. Simon, O. Zilberberg, and I. Carusotto, Topological photonics, *Rev. Mod. Phys.* **91**, 015006 (2019).
- [27] M. Aspelmeyer, T. J. Kippenberg, and F. Marquardt, Cavity optomechanics, *Rev. Mod. Phys.* **86**, 1391 (2014).
- [28] S. D. Huber, Topological mechanics, *Nature Physics* **12**, 621 (2016).
- [29] S. Walter and F. Marquardt, Classical dynamical gauge fields in optomechanics, *New Journal of Physics* **18**, 113029 (2016).
- [30] O. Dutta, M. Gajda, P. Hauke, M. Lewenstein, D.-S. Lühmann, B. A. Malomed, T. Sowinski, and J. Zakrzewski, Non-standard Hubbard models in optical lattices: a review, *Reports on Progress in Physics* **78**, 066001 (2015).
- [31] T. Chanda, L. Barbiero, M. Lewenstein, M. J. Mark, and J. Zakrzewski, Recent progress on quantum simulations of non-standard Bose-Hubbard models (2024), [arXiv:2405.07775 \[cond-mat.quant-gas\]](https://arxiv.org/abs/2405.07775).
- [32] S. Asban and S. Mukamel, Scattering-based geometric shaping of photon-photon interactions, *Phys. Rev. Lett.* **123**, 260502 (2019).
- [33] D. Lewis, A. Benhemou, N. Feinstein, L. Banchi, and S. Bose, Optimal quantum spatial search with one-dimensional long-range interactions, *Phys. Rev. Lett.* **126**, 240502 (2021).
- [34] E. C. King, M. Linnebacher, P. P. Orth, M. Rizzi, and G. Morigi, Optimal spatial searches with long-range tunneling (2025), [arXiv:2501.08148 \[quant-ph\]](https://arxiv.org/abs/2501.08148).
- [35] B. M. Weight, X. Li, and Y. Zhang, Theory and modeling of light-matter interactions in chemistry: current and future, *Phys. Chem. Chem. Phys.* **25**, 31554 (2023).
- [36] Supplemental material, URL will be inserted by publisher.
- [37] H. Ritsch, P. Domokos, F. Brennecke, and T. Esslinger, Cold atoms in cavity-generated dynamical optical potentials, *Rev. Mod. Phys.* **85**, 553 (2013).
- [38] A. Forbes, A. Dudley, and M. McLaren, Creation and detection of optical modes with spatial light modulators, *Adv. Opt. Photon.* **8**, 200 (2016).
- [39] O. Katz and C. Monroe, Programmable quantum simulations of bosonic systems with trapped ions, *Phys. Rev. Lett.* **131**, 033604 (2023).
- [40] M. Sato, S. Furukawa, S. ONODA, and A. FURUSAKI, Competing phases in spin-1/2  $j_1$ - $j_2$  chain with easy-plane anisotropy, *Modern Physics Letters B* **25**, 901 (2011), <https://doi.org/10.1142/S0217984911026607>.
- [41] J. Struck, Quantum simulation of frustrated classical magnetism in triangular optical lattices, *Science* **333**, 996 (2011), <https://www.science.org/doi/pdf/10.1126/science.1207239>.
- [42] D. T. Son and P. Surówka, Hydrodynamics with triangle anomalies, *Phys. Rev. Lett.* **103**, 191601 (2009).
- [43] B. Damski, H. Fehrmann, H.-U. Everts, M. Baranov, L. Santos, and M. Lewenstein, Quantum gases in trimerized kagomé lattices, *Phys. Rev. A* **72**, 053612 (2005).
- [44] A. Eckardt, P. Hauke, P. Soltan-Panahi, C. Becker, K. Sengstock, and M. Lewenstein, Frustrated quantum antiferromagnetism with ultracold bosons in a triangular lattice, *EPL* **89**, 10010 (2010).
- [45] T. Zhang and G.-B. Jo, One-dimensional sawtooth and zigzag lattices for ultracold atoms, *Sci. Rep.* **5**, 16044 (2015).
- [46] E. Anisimovas, M. Račiūnas, C. Sträter, A. Eckardt, I. B. Spielman, and G. Juzeliūnas, Semisynthetic zigzag optical lattice for ultracold bosons, *Phys. Rev. A* **94**, 063632 (2016).
- [47] J. Cabedo, J. Claramunt, J. Mompart, V. Ahufinger, and A. Celi, Effective triangular ladders with staggered flux from spin-orbit coupling in 1D optical lattices, *The European Physical Journal D* **74**, 123 (2020).
- [48] L. Barbiero, J. Cabedo, M. Lewenstein, L. Tarruell, and A. Celi, Frustrated magnets without geometrical frustration in bosonic flux ladders, *Phys. Rev. Res.* **5**, L042008 (2023).
- [49] N. Baldelli, C. R. Cabrera, S. Julià-Farré, M. Aidelsburger, and L. Barbiero, Frustrated extended Bose-Hubbard model and de-

- confined quantum critical points with optical lattices at the antimagical wavelength, *Phys. Rev. Lett.* **132**, 153401 (2024).
- [50] D. Burba, G. Juzeliūnas, I. B. Spielman, and L. Barbiero, Many-body phases from effective geometrical frustration and long-range interactions in a subwavelength lattice (2024), arXiv:2409.01443 [cond-mat.quant-gas].
- [51] Z. Zhu and S. R. White, Spin liquid phase of the  $s = \frac{1}{2} J_1 - J_2$  heisenberg model on the triangular lattice, *Phys. Rev. B* **92**, 041105 (2015).
- [52] L. Balents, Spin liquids in frustrated magnets, *Nature* **464**, 199–208 (2010).
- [53] K. Kim, M.-S. Chang, R. Islam, S. Korenblit, L.-M. Duan, and C. Monroe, Entanglement and tunable spin-spin couplings between trapped ions using multiple transverse modes, *Phys. Rev. Lett.* **103**, 120502 (2009).
- [54] J. W. Britton, B. C. Sawyer, A. C. Keith, C.-C. J. Wang, J. K. Freericks, H. Uys, M. J. Biercuk, and J. J. Bollinger, Engineered two-dimensional ising interactions in a trapped-ion quantum simulator with hundreds of spins, *Nature* **484**, 489–492 (2012).
- [55] R. Islam, C. Senko, W. C. Campbell, S. Korenblit, J. Smith, A. Lee, E. E. Edwards, C.-C. J. Wang, J. K. Freericks, and C. Monroe, Emergence and frustration of magnetism with variable-range interactions in a quantum simulator, *Science* **340**, 583–587 (2013).
- [56] Quasiparticle engineering and entanglement propagation in a quantum many-body system, *Nature* **511**, 202 (2014).
- [57] C. Kokail, C. Maier, R. van Bijnen, T. Brydges, M. K. Joshi, P. Jurcevic, C. A. Muschik, P. Silvi, R. Blatt, C. F. Roos, and P. Zoller, Self-verifying variational quantum simulation of lattice models, *Nature* **569**, 355 (2019).
- [58] L. K. Grover, A fast quantum mechanical algorithm for database search, in *Proceedings of the Twenty-Eighth Annual ACM Symposium on Theory of Computing*, STOC '96 (Association for Computing Machinery, New York, NY, USA, 1996) p. 212–219.
- [59] L. K. Grover, Quantum mechanics helps in searching for a needle in a haystack, *Phys. Rev. Lett.* **79**, 325 (1997).
- [60] F. D. M. Haldane, Model for a quantum hall effect without landau levels: Condensed-matter realization of the "parity anomaly", *Phys. Rev. Lett.* **61**, 2015 (1988).
- [61] D. E. Chang, V. Vuletic, and M. D. Lukin, Quantum nonlinear optics – photon by photon, *Nature Photonics* **8**, 685 (2014).
- [62] I. Carusotto, A. A. Houck, A. Kollar, P. Roushan, D. S. Schuster, and J. Simon, Photonic materials in circuit quantum electrodynamics, *Nature Physics* **16**, 268 (2020).
- [63] A. Aiello and J. P. Woerdman, Exact quantization of a paraxial electromagnetic field, *Phys. Rev. A* **72**, 060101 (2005).

## SUPPLEMENTAL MATERIAL

In this Supplemental material, we give additional information about the main techniques employed in the main text, as well as calculation steps that were not considered crucial for the comprehension of the results.

### Effective many-body Hamiltonian

In this section, we systematically derive the effective Hamiltonian of Eq. (8).

We write the Hamiltonian as

$$\mathcal{H} = \underbrace{\sum_{\alpha} \left( \frac{\vec{p}_{\alpha}^2}{2m} + V(\vec{r}_{\alpha}) \right) + \omega_0 \sum_n b_n^{\dagger} b_n}_{=:H_0} \quad (14)$$

$$+ \underbrace{\sum_{\alpha} \frac{e^2}{2mc^2} \vec{A}(\vec{r}_{\alpha})^2 + \sum_n \delta_n b_n^{\dagger} b_n}_{=:H_1}, \quad (15)$$

where  $\delta_n = \omega_n - \omega_0$  are small corrections for the frequencies of the modes in the expansion of the EM part of the Hamiltonian. In our case, these modes are chosen to be eigenmodes of the paraxial Helmholtz equation [63].

Assuming that each molecule is a two-level system with ground state  $|g_{\alpha}\rangle$  and excited state  $|e_{\alpha}\rangle$ , and a gap  $E = \Delta$ , the unperturbed part  $H_0$  can easily be diagonalized and the Hamiltonian takes the form

$$\mathcal{H}_0 = \sum_{\alpha} \Delta |e_{\alpha}\rangle \langle e_{\alpha}| + \omega_0 \sum_n b_n^{\dagger} b_n, \quad (16)$$

$$\mathcal{H}_1 = \sum_n \delta_n b_n^{\dagger} b_n + \sum_{\alpha} \frac{e^2}{2mc^2} \vec{A}(\vec{r}_{\alpha})^2. \quad (17)$$

The EM part of the Hamiltonian is diagonalized by eigenmodes of the Maxwell equations, and in the following, we work in the sector of constant photon number. Our theoretical considerations go beyond the dipolar approximation, and therefore, the vector potential acts non-trivially on the molecular eigenstates.

We proceed by calculating the effective Hamiltonian for the EM modes in second order perturbation theory, where the perturbation Hamiltonian is  $\mathcal{H}_1$ .

## Hopping term amplitudes

The first order correction to the energy is given by

$$\begin{aligned} & \frac{e^2}{2mc^2} \sum_{\alpha} \langle g_{\alpha} | \vec{A}(\vec{r}_{\alpha})^2 | g_{\alpha} \rangle + \sum_n \delta_n b_n^{\dagger} b_n \\ &= \frac{e^2}{2mc^2} \sum_{\alpha, n, m} \left( \langle g_{\alpha} | f_n(\vec{r}_{\alpha}) f_m^*(\vec{r}_{\alpha}) | g_{\alpha} \rangle b_n^{\dagger} b_m + \text{h.c.} \right) \\ &+ \sum_n \delta_n b_n^{\dagger} b_n \\ &\equiv \sum_{n, m} (t_{nm} b_n^{\dagger} b_m + \text{h.c.}) + \sum_n \delta_n b_n^{\dagger} b_n, \end{aligned} \quad (18)$$

where we defined

$$t_{nm} = \frac{e^2}{2mc^2} \sum_{\alpha} \langle g_{\alpha} | f_n(\vec{r}_{\alpha}) f_m^*(\vec{r}_{\alpha}) | g_{\alpha} \rangle \quad (19)$$

We further switch from discrete description of the molecules to a continuous one,  $\sum_{\alpha} \rightarrow \int_V d^3r \rho(\vec{r})$ . The volume  $V$  is determined by the total volume of the molecular cloud. The coefficients  $t_{nm}$  become

$$t_{nm} = \int_V d^3r \rho(\vec{r}) f_n(\vec{r}) f_m^*(\vec{r}). \quad (20)$$

Therefore, the diagonal part of the perturbation to the energy is

$$\mathcal{H} = \sum_n t_{nn} b_n^{\dagger} b_n + \sum_n \delta_n b_n^{\dagger} b_n \equiv \sum_n \mu_n b_n^{\dagger} b_n \quad (21)$$

and the off-diagonal, which corresponds to the hopping amplitudes between different modes,

$$\mathcal{H} = \sum_{n, m} t_{nm} b_n^{\dagger} b_m + \text{h.c.} \quad (22)$$

### Density-density interactions

The second order correction to the energy is given by

$$\begin{aligned} & - \frac{1}{\Delta} \left( \frac{e^2}{2mc^2} \right)^2 \sum_{\alpha} | \langle g_{\alpha} | \vec{A}(\vec{r}_{\alpha})^2 | e_{\alpha} \rangle |^2 \\ &= - \frac{1}{\Delta} \left( \frac{e^2}{2mc^2} \right)^2 \sum_{\alpha} | \langle g_{\alpha} | \sum_{n, m} f_n(\vec{r}_{\alpha}) f_m^*(\vec{r}_{\alpha}) | e_{\alpha} \rangle |^2 \end{aligned} \quad (23)$$

As we mentioned in the main text, we now rewrite the off-diagonal element of the vector potential as proportional to the diagonal one with proportionality factor  $\nu$ ; using Eq. (6) we



obtain

$$\begin{aligned}
& \sum_{\alpha} |\langle g_{\alpha} | \vec{A}(\vec{r}_{\alpha})^2 | e_{\alpha} \rangle|^2 \\
&= \nu^2 \sum_{\alpha} |\langle g_{\alpha} | \sum_{n,m} f_n(\vec{r}_{\alpha}) f_m^*(\vec{r}_{\alpha}) b_n^{\dagger} b_m + \text{h.c.} | g_{\alpha} \rangle|^2 \\
&= \nu^2 \sum_{\alpha} \langle g_{\alpha} | \sum_{n,m,n',m'} f_n(\vec{r}_{\alpha}) f_m^*(\vec{r}_{\alpha}) f_{n'}(\vec{r}_{\alpha}) f_{m'}^*(\vec{r}_{\alpha}) \\
&\quad \times b_n^{\dagger} b_m b_{n'}^{\dagger} b_{m'} | g_{\alpha} \rangle \\
&+ \nu^2 \sum_{\alpha} \langle g_{\alpha} | \sum_{n,m,n',m'} f_n(\vec{r}_{\alpha}) f_m^*(\vec{r}_{\alpha}) f_{n'}^*(\vec{r}_{\alpha}) f_{m'}(\vec{r}_{\alpha}) \\
&\quad \times b_n^{\dagger} b_m b_{n'} b_{m'}^{\dagger} | g_{\alpha} \rangle \\
&+ \text{h.c.} \tag{24}
\end{aligned}$$

Replacing the discrete description of the molecular cloud with a continuous one, we obtain for the second order correction

$$\begin{aligned}
& -\frac{1}{\Delta} \left( \frac{e^2}{2mc^2} \right)^2 \sum_{\alpha} |\langle g_{\alpha} | \vec{A}(\vec{r}_{\alpha})^2 | e_{\alpha} \rangle|^2 \\
&= -\sum_{m,n} U_{mn} (4b_n^{\dagger} b_n b_m^{\dagger} b_m + 3b_n^{\dagger} b_n), \tag{25}
\end{aligned}$$

where we defined the interaction strength

$$U_{mn} = \frac{\nu^2}{\Delta} \left( \frac{e^2}{2mc^2} \right)^2 \int_V d^3\vec{r} \rho(\vec{r}) |f_n(\vec{r})|^2 |f_m(\vec{r})|^2. \tag{26}$$

It should be noted that the right-hand side of Eq. (24) contains additional terms beyond the ones in Eq. (25). However, these additional terms can be neglected since the LG modes carry a non-trivial time-dependent phase factor due to their small energy shifts  $\delta_n$ . Therefore, only those terms survive a time averaging, for which these phase factors exactly cancel out.

## Laguerre-Gaussian modes

As we explained in the main text, the set of EM eigenmodes used in this Letter is the Laguerre-Gaussian modes, due to the cylinder symmetry of the considered setup. The spatial profile of these modes is given by

$$\begin{aligned}
f_{l,p}(\vec{r}) &= \left( \frac{\hbar}{8\pi^2 \epsilon_0 \omega_0 (1 + \vartheta^4)^{1/2} L} \right)^{1/2} \frac{C_{l,p}}{w(z)} \left( \frac{r\sqrt{2}}{w(z)} \right)^{|l|} \\
&\quad \times \exp \left( -\frac{r^2}{w^2(z)} \right) L_p^{|l|} \left( \frac{2r^2}{w^2(z)} \right) \\
&\quad \times \exp \left( -ik_0 \frac{r^2}{2R(z)} \right) \exp(-il\phi) \exp[i\psi(z)], \tag{27}
\end{aligned}$$

where  $w(z)$  is the waist radius,  $R(z)$  the radius of curvature,  $k = 2\pi/\lambda$  the wave-number for the wavelength  $\lambda$  and  $\psi(z)$  is the Gouy phase. In the prefactor, the  $\epsilon_0$  is the vacuum dielectric permittivity,  $\vartheta$  is the (small) divergence angle of the Gaussian beam and  $L$  is the extent of the cavity along the  $z$ -direction. The coefficient  $C_{l,p}$  is a normalization constant

$$C_{l,p} = \sqrt{\frac{2p!}{\pi(p+|l|)!}}, \tag{28}$$

so that the orthogonality condition

$$\int d^3\vec{r} f_{l,p}(\vec{r}) f_{l',p'}(\vec{r}) = \delta_{l,l'} \delta_{p,p'} \tag{29}$$

and the normalization condition

$$\int d^3\vec{r} |f_{l,p}(\vec{r})|^2 = 1 \tag{30}$$

hold. We simplify the description by assuming small divergence of the beam along the  $z$ -direction and therefore, in cylindrical coordinates, the integrals defining the coefficients of the effective Hamiltonian along that direction are rather trivial (see Eq. (11)). The integration in the plane perpendicular to  $z$  is non-trivial and we perform it numerically.